

Correspondence

A New Formula for Lognormal Characteristic Functions

John A. Gubner

Abstract—Numerical computation of lognormal characteristic functions is a challenging problem because the defining integral formulas are not well suited to the more common numerical integration techniques. In this paper, a simple change-of-contour argument is used to convert the integral into one in which the oscillatory nature of the new integrand does not depend on the argument of the characteristic function. Hence, efficient numerical computation of the characteristic function is possible for an extremely large range of its argument. The method generalizes to allow the computation of the moment-generating function when the argument has a negative real part. A simple program for computing the new integral using Gaussian quadrature and another program for generating the quadrature nodes and weights are given.

Index Terms—Approximation methods, Fourier transforms, Gaussian quadrature, moment-generating function, numerical integration.

I. INTRODUCTION

Computation of lognormal characteristic functions is a challenging problem because no closed-form expression exists [10] and because the defining integral formulas are not well suited to the more common numerical integration techniques [5]. This is unfortunate because the characteristic function would be the obvious tool for analyzing sums of independent lognormal random variables.

The study of such sums has been of intense interest in the study of radio transmission, at least as far back as the 1960 paper of Fenton [8]. Fenton noted that the numerical convolution of two lognormal densities resembled another lognormal density. This appears to be the starting point for him and for subsequent authors to study the approximation of the distribution of a sum of lognormal random variables by a lognormal distribution, e.g., [2]–[6], [13], and [14].

In particular, the 2004 paper of Beaulieu and Xie [5] summarizes the advantages and disadvantages of various methods. To assess these approximations, Beaulieu and Xie first needed to compute lognormal characteristic functions, which is very challenging. They tried a number of techniques such as the trapezoidal rule, Simpson's rule, and the fast Fourier transform, and finally settled on the modified Clenshaw–Curtis method [12].

In this paper, we regard the characteristic function as a contour integral of an entire function in the complex plane. By the Cauchy–Goursat theorem, we are justified in using an alternative contour. We propose a new contour that has the advantage of the oscillatory nature of the resulting integrand not depending on the argument of the characteristic function. Hence, we can readily compute the characteristic function for an extremely large range of its argument numerically, e.g., $0 \leq \nu \leq 10\,000$. This is illustrated using the characteristic functions considered in [5].

Manuscript received June 2, 2005; revised October 19, 2005 and January 16, 2006. The review of this paper was coordinated by Prof. Y. Ma.

The author is with the Department of Electrical and Computer Engineering, University of Wisconsin, Madison, WI 53706-1691 USA (e-mail: gubner@engr.wisc.edu).

Digital Object Identifier 10.1109/TVT.2006.878610

Remark: Our method generalizes to allow the computation of the moment-generating function when its argument has a negative real part. Details are presented at the end of Section III.

II. NOTATION

Let $Z \sim N(0, \sigma^2)$ denote a Gaussian random variable with zero mean and variance σ^2 , i.e., the density of Z is

$$f(z) := \frac{\exp[-(z/\sigma)^2/2]}{\sqrt{2\pi}\sigma}.$$

The random variable $Y := e^Z$ is said to be lognormal. It follows that the lognormal characteristic function is

$$\varphi(\nu) := \mathbb{E}[e^{j\nu Y}] = \mathbb{E}[\exp\{j\nu e^Z\}].$$

As noted in [11, eq. (14)] and [5, p. 481], there is no loss of generality in assuming that Z has zero mean; just observe that for any constant m

$$\mathbb{E}[\exp\{j\nu e^{(Z+m)}\}] = \mathbb{E}[\exp\{j(\nu e^m)e^Z\}] = \varphi(\nu e^m).$$

Recall also that $\varphi(0) = 1$, $\text{Re } \varphi$ is even, and $\text{Im } \varphi$ is odd; hence, it suffices to restrict attention to $\nu > 0$.

The dB spread of Y , which is denoted by σ_{dB} , is defined as the standard deviation of

$$10 \log_{10} Y = \frac{10}{\ln(10)} Z.$$

Hence, $\sigma_{\text{dB}} = \sigma \cdot 10/\ln(10)$, or $\sigma = \sigma_{\text{dB}} \ln(10)/10$.

III. NEW FORMULA FOR THE LOGNORMAL CHARACTERISTIC FUNCTION

From the preceding discussion, we have

$$\varphi(\nu) = \mathbb{E}[\exp\{j\nu e^Z\}] = \int_{-\infty}^{\infty} \exp\{j\nu e^z\} f(z) dz. \quad (1)$$

This integral is notoriously difficult to compute numerically because the factor $\exp\{j\nu e^z\}$ is extremely oscillatory as $z \rightarrow +\infty$. Furthermore, as σ increases, the width of the Gaussian density $f(z)$ increases, and more oscillations have to be considered. An obvious alternative is to make the change of variable $\tau = e^z$. This results in an ordinary Fourier transform integral of $f(\ln \tau)/\tau$ from zero to infinity. However, the function $f(\ln \tau)/\tau$ decays very slowly, and so, there are still excessively many oscillations to be considered.

We propose another approach as follows: First, the integral in (1) can be viewed as a contour integral in the complex plane with the contour being the real axis. Second, the integrand is an entire function. Third, using the Cauchy–Goursat theorem [7], it is easy to argue that for $\nu > 0$, the previous integral is equal to

$$\int_C \exp\{j\nu e^z\} f(z) dz$$

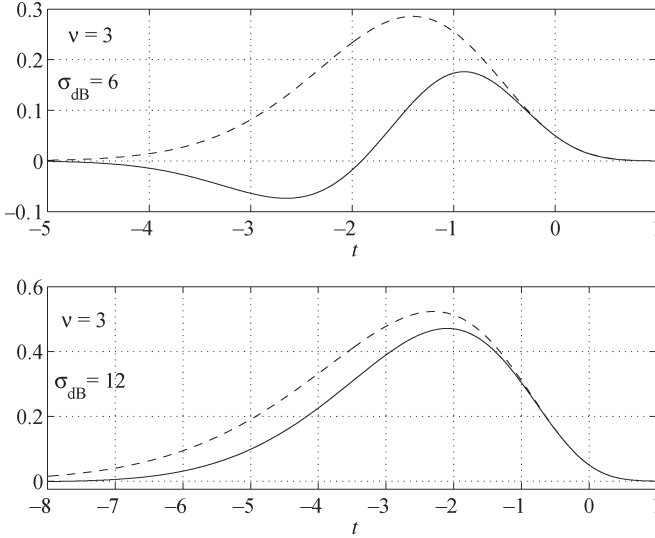


Fig. 1. Dashed lines show the envelope $\exp[-\{\nu e^t + (t/\sigma)^2/2\}]$, and the solid lines show the real part of the integrand in (2).

where C is the contour

$$C := \{z(t) = t + j\pi/2 : -\infty < t < \infty\}.$$

Thus, we have

$$\varphi(\nu) = \frac{\exp[(\pi/(2\sigma))^2/2]}{\sqrt{2\pi}\sigma} \cdot \int_{-\infty}^{\infty} \exp[-\nu e^t] e^{-j\pi t/(2\sigma^2)} e^{-(t/\sigma)^2/2} dt. \quad (2)$$

Notice that now the only oscillatory factor $e^{-j\pi t/(2\sigma^2)}$ does not depend on ν and depends only linearly on t . As σ increases, the oscillations become less, as illustrated in Fig. 1, making numerical integration easier.

The foregoing change-of-contour method easily generalizes to compute the moment-generating function $E[e^{sY}]$ for $\text{Re } s < 0$. In this case, if $s = \lambda + j\nu$, the new contour would be

$$C = \{z(t) = t + j\theta, -\infty < t < \infty\}$$

where $\theta := \tan^{-1}(-\nu/\lambda)$. The resulting integral is

$$E[e^{(\lambda+j\nu)Y}] = \frac{\exp[(\theta/\sigma)^2/2]}{\sqrt{2\pi}\sigma} \cdot \int_{-\infty}^{\infty} \exp[e^t(\lambda \cos \theta - \nu \sin \theta)] \cdot e^{-j\theta t/\sigma^2} e^{-(t/\sigma)^2/2} dt.$$

The only oscillating factor is $e^{-j\theta t/\sigma^2}$. Although θ depends on λ and ν , $0 \leq |\theta| < \pi/2$. Hence, the oscillations of the integrand cannot get arbitrarily bad.

IV. FAST COMPUTATION OF (2)

Make the change of variable $x = t/(\sqrt{2}\sigma)$ in (2) to get

$$\varphi(\nu) = \frac{\exp[(\pi/(2\sigma))^2/2]}{\sqrt{\pi}} \psi(\nu) \quad (3)$$

where

$$\psi(\nu) := \int_{-\infty}^{\infty} \exp[-\nu e^{\sqrt{2}\sigma x}] e^{-j\pi x/(\sqrt{2}\sigma)} e^{-x^2} dx. \quad (4)$$

Using n -point Hermite–Gauss quadrature [1], [9] with weights w_k and nodes x_k , we have

$$\psi(\nu) \approx \sum_{k=1}^n w_k \exp[-\nu e^{\sqrt{2}\sigma x_k}] e^{-j\pi x_k/(\sqrt{2}\sigma)}.$$

A six-line Matlab program is given in the Appendix for generating the Hermite–Gauss weights w_k and nodes x_k .

Example 1: It is easy to evaluate the preceding formula in Matlab using vectorized code and then apply (3). Let \mathbf{w} denote the row vector of the weights, and let \mathbf{x} denote the column vector of the nodes for n -point Hermite–Gauss quadrature. Suppose that \mathbf{nu} is a row vector of points ν at which we need to compute $\varphi(\nu)$. Then, the following Matlab script computes the row vector of values $\varphi(\nu)$ and plots the real and imaginary parts:

```
% Get nodes and weights (see Appendix).
[x, w] = hermitequad(45);
%
% Precompute all quantities not
% depending on nu.
%
sigma = 0.25;
sqrt2 = sqrt(2);
Hfactor = exp((pi/2/sigma)^2/2)/sqrt(pi);
wej = w * exp(-j * pi/sqrt2/sigma * x');
exparg = exp(sqrt2 * sigma * x);
%
% Compute phi(nu) and plot.
%
nu = linspace(0, 20, 200);
phi = ones(size(nu));
I = find(nu == 0);
phi(I) = Hfactor * wej * exp(-exparg * nu(I));
plot(nu, real(phi), nu, imag(phi), 'r');
```

Such plots are shown in Figs. 2–4 for $\sigma = 0.25$, $\sigma_{\text{dB}} = 6$ (corresponding to $\sigma \approx 1.38$), and $\sigma_{\text{dB}} = 12$ (corresponding to $\sigma \approx 2.76$), respectively. All the plots were generated with ($n = 45$)-point Hermite–Gauss quadrature. The plots agree with [5, Figs. 1–3]. Increasing n beyond 45 did not visually change our plots.

Example 2: Because the oscillatory behavior of the integrand in (2) does not depend on ν , we can compute $\varphi(\nu)$ for extremely large values of ν . This is illustrated in Figs. 5 and 6 still using ($n = 45$)-point Hermite–Gauss quadrature. These plots show on a semilog scale the absolute values of the real and imaginary parts of $\varphi(\nu)$ for $\sigma_{\text{dB}} = 6$ and $\sigma_{\text{dB}} = 12$. The cusps occur at the roots of the functions.

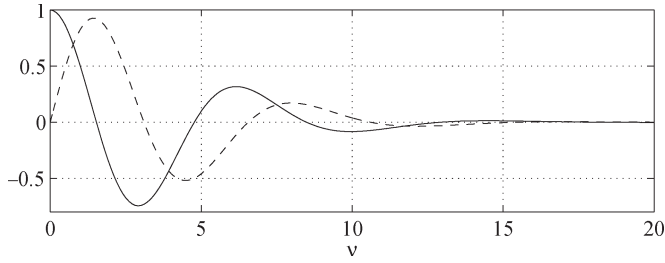


Fig. 2. Real part (solid line) and imaginary part (dashed line) of characteristic function $\phi(\nu)$ with $\sigma = 0.25$.

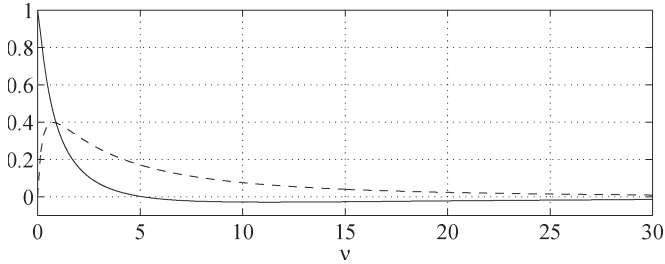


Fig. 3. Real part (solid line) and imaginary part (dashed line) of characteristic function $\phi(\nu)$ with $\sigma_{\text{dB}} = 6$ ($\sigma \approx 1.38$).

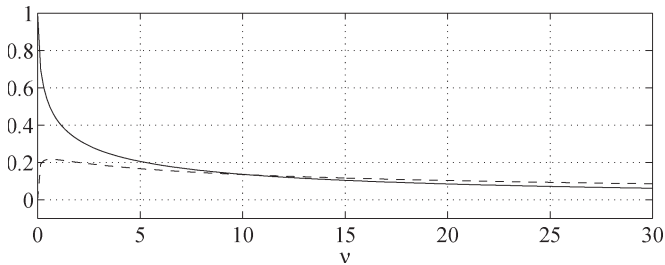


Fig. 4. Real part (solid line) and imaginary part (dashed line) of characteristic function $\phi(\nu)$ with $\sigma_{\text{dB}} = 12$ ($\sigma \approx 2.76$).

V. MORE ACCURATE COMPUTATION OF (2)

Basic calculus applied to the exponent of the envelope $\exp[-\{\nu e^t + (t/\sigma)^2/2\}]$ in (2) shows that the envelope maximum occurs at the solution of $e^t = -t/(\nu\sigma^2)$. Denote this solution by t_0 . Sketching the curve e^t and the straight line $-t/(\nu\sigma^2)$ shows that the solution t_0 is always negative and goes to $-\infty$ as the product $\nu\sigma^2$ goes to ∞ . It is easy to obtain t_0 using the Matlab function `fzero`.

The nodes for Hermite–Gauss quadrature are centered around the origin. However, as the product $\nu\sigma^2$ becomes large, the “important” part of the integrand drifts off to the left. Hence, a better approximation of (2) can be obtained if the infinite limits of integration are replaced with finite limits a and b , with $a < t_0 < b$ and such that the envelope at a and at b is, say, 10^{-16} of the maximum envelope value at t_0 . In other words, a and b are the solutions of

$$\exp[-\{\nu e^t + (t/\sigma)^2/2\}] = \exp[-\{\nu e^{t_0} + (t_0/\sigma)^2/2\}] / 10^{16}.$$

Taking logarithms, we see that a and b are the solutions of

$$\nu e^t + (t/\sigma)^2/2 - \{\nu e^{t_0} + (t_0/\sigma)^2/2\} - 16 \ln 10 = 0.$$

Hence, a and b are also easily obtained using `fzero`.

Next, any integral over $[a, b]$ is easily written as an integral over $[0, 1]$, and integrals over $[0, 1]$ are easily approximated using the

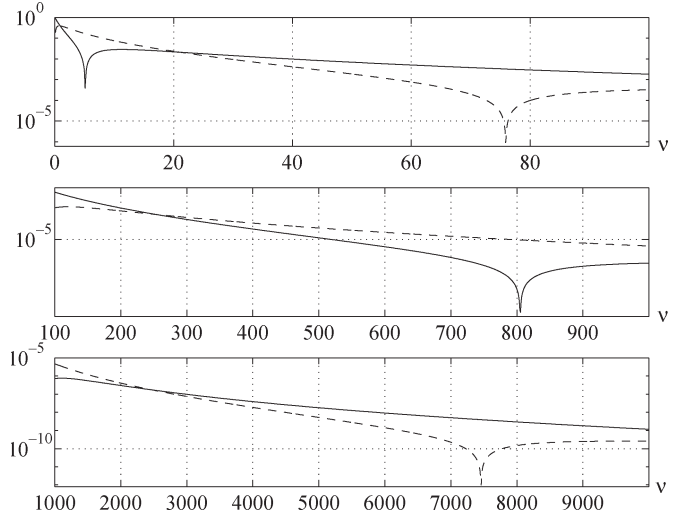


Fig. 5. Absolute values of the real part (solid line) and imaginary part (dashed line) of characteristic function $\phi(\nu)$ with $\sigma_{\text{dB}} = 6$ ($\sigma \approx 1.38$).

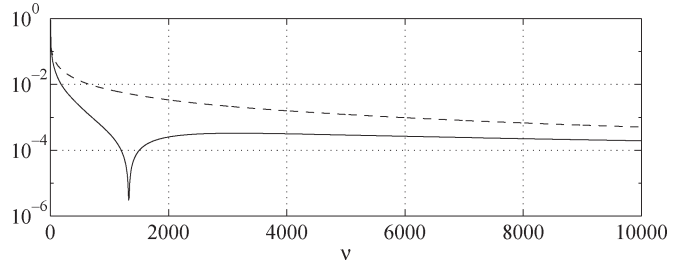


Fig. 6. Absolute values of the real part (solid line) and imaginary part (dashed line) of characteristic function $\phi(\nu)$ with $\sigma_{\text{dB}} = 12$ ($\sigma \approx 2.76$).

Legendre–Gauss quadrature. As noted in the Appendix, a trivial modification to the Matlab function found there will return the nodes and weights necessary for Legendre–Gauss quadrature.

Example 3: With $\sigma_{\text{dB}} = 12$ and $\nu = 10000$, we computed $\varphi(\nu)$ using 45-point Hermite–Gauss quadrature and 45-point Legendre–Gauss quadrature after determining $a = -25.7$, $t_0 = -9.04$, and $b = -5.49$. The results are (real part only)

$$\varphi(\nu) = \begin{cases} -1.93 \times 10^{-4}, & \text{(Hermite–Gauss)} \\ -1.9300709586 \times 10^{-4}, & \text{(Legendre–Gauss)} \end{cases}$$

which are correct to the number of digits shown. In both methods, more correct digits can be obtained by increasing the number of quadrature nodes and weights. However, for a given amount of integration work, applying that work to the interval $[a, b]$ yields better results.

VI. CONCLUSION

We have derived a new integral formula (2) for the lognormal characteristic function. It has the advantage of the oscillations in the integrand no longer depending on the argument of the characteristic function. The new integral is well suited to Gaussian quadrature, and we have provided a simple Matlab function in the Appendix to compute the nodes and weights. Our new integral becomes better suited for numerical computation as σ increases. We also note that as $\sigma \rightarrow 0$, factor in (3) goes to infinity. However, for a small σ , Hermite–Gauss quadrature can be applied directly to (1).

APPENDIX

The Matlab function shown below generates Hermite–Gauss nodes and weights. The program is based on the following result, which can be found in [9, p. 153].

Theorem: The nodes x_i and weights w_i of a Gaussian quadrature formula based on orthogonal polynomials can be obtained from the eigenvalue decomposition of the symmetric tridiagonal Jacobi matrix

$$J_n := \begin{bmatrix} a_0 & \sqrt{b_1} & & & & \\ \sqrt{b_1} & a_1 & \sqrt{b_2} & & & \\ & \sqrt{b_2} & \ddots & \ddots & & \\ & & \ddots & a_{n-2} & \sqrt{b_{n-1}} & \\ & & & \sqrt{b_{n-1}} & a_{n-1} & \end{bmatrix}$$

where a_n and b_n are the same as those in the three-term recurrence formula for the orthogonal polynomials normalized to have leading coefficient one. If $V'J_nV = \Lambda = \text{diag}(\lambda_1, \dots, \lambda_n)$, where $V'V = I$ is the $n \times n$ identity matrix, then $x_i = \lambda_i$, and $w_i = b_0 v_{i,1}^2$, where v_i is the i th column of V , and $v_{i,1}$ is the first component of v_i .

For the Hermite polynomials with leading coefficient one, we have from [9, p. 29, Table 1.1] that for $k = 1, 2, \dots, a_k = 0$ and $b_k = k/2$; we also have $b_0 = \sqrt{\pi}$. Hence, the following Matlab function is immediate:

```
function [x,w] = hermitequad(n)
%
% Generate nodes and weights for
% Hermite-Gauss quadrature.
% Note that x is a column vector
% and w is a row vector.
%
u = sqrt([1:n-1]/2); % upper diagonal of J
[V,Lambda] = eig(diag(u,1) + diag(u,-1));
[x,i] = sort(diag(Lambda));
Vtop = V(1,:);
Vtop = Vtop(i);
w = sqrt(pi) * Vtop.^2;
```

Remark: Using [9, p. 29, Table 1.1], it is trivial to modify the preceding Matlab code to return the nodes and weights for other quadratures such as Laguerre–Gauss and Legendre–Gauss.

REFERENCES

- [1] M. Abramowitz and I. A. Stegun, Eds., *Handbook of Mathematical Functions, With Formulas, Graphs, and Mathematical Tables*. New York: Dover, 1970.
- [2] N. C. Beaulieu, A. A. Abu-Dayya, and P. J. McLane, "Comparison of methods of computing lognormal sum distributions and outages for digital wireless applications," in *Proc. IEEE ICC*, New Orleans, LA, Jun. 1994, pp. 1270–1275.
- [3] —, "Estimating the distribution of a sum of independent lognormal random variables," *IEEE Trans. Commun.*, vol. 43, no. 12, pp. 2869–2873, Dec. 1995.
- [4] N. C. Beaulieu and F. Rajwani, "Highly accurate simple closed-form approximations to lognormal sum distributions and densities," *IEEE Commun. Lett.*, vol. 8, no. 12, pp. 709–711, Dec. 2004.
- [5] N. C. Beaulieu and Q. Xie, "An optimal lognormal approximation to lognormal sum distributions," *IEEE Trans. Veh. Technol.*, vol. 53, no. 2, pp. 479–489, Mar. 2004.
- [6] P. Cardieri and T. S. Rappaport, "Statistics of the sum of lognormal variables in wireless communications," in *Proc. IEEE Veh. Technol. Conf.*, Tokyo, Japan, 2000, vol. 3, pp. 1823–1827.
- [7] R. V. Churchill, J. W. Brown, and R. F. Verhey, *Complex Variables and Applications*, 3rd ed. New York: McGraw-Hill, 1976.
- [8] L. F. Fenton, "The sum of log-normal probability distributions in scatter transmission systems," *IRE Trans. Commun. Syst.*, vol. CS-8, no. 1, pp. 57–67, Mar. 1960.
- [9] W. Gautschi, *Orthogonal Polynomials: Computation and Approximation*. Oxford, U.K.: Oxford Univ. Press, 2004.
- [10] N. L. Johnson, S. Kotz, and N. Balakrishnan, *Continuous Univariate Distributions*, 2nd ed, vol. 1. New York: Wiley, 1994.
- [11] R. B. Leipnik. (1991). On lognormal random variables—Part I: The characteristic function. *J. Aust. Math. Soc. Series B*. [Online]. 32(pt. 3), pp. 327–347. Available: <http://anziamj.austms.org.au/V32/part3/Leipnik.html>
- [12] R. Piessens, E. de Doncker-Kapenga, C. W. Überhuber, and D. K. Kahaner, *Quadpack: A Subroutine Package for Automatic Integration*. Berlin, Germany: Springer-Verlag, 1983.
- [13] S. C. Schwartz and Y. S. Yeh, "On the distribution function and moments of power sums with lognormal components," *Bell Syst. Tech. J.*, vol. 61, no. 7, pp. 1441–1462, Sep. 1982.
- [14] S. B. Slimane, "Bounds on the distribution of a sum of independent lognormal random variables," *IEEE Trans. Commun.*, vol. 49, no. 6, pp. 975–978, Jun. 2001.

Steered-STS Transmit Antenna Architecture With Semiblind Channel Estimation at the Receiver in CDMA2000

Alexandr M. Kuzminskiy, Francis J. Mullany, and
Constantinos B. Papadias

Abstract—The problem of pilot and data channel mismatch in a steered space-time spreading (SSTS) system is addressed by means of advanced signal processing at the mobile receiver. The main idea is to apply the SSTS antenna array architecture and transmission algorithm and involve both the pilot and traffic signals in channel estimation at the receiver. Two semiblind algorithms are compared with the conventional pilot-based receiver in a CDMA2000-1X RC3 environment by means of simulations with variable speed and spatial angular spread, taking into account main imperfections such as estimation error for the correlation coefficient at the reverse link, calibration error, and different pilot powers for diversity antennas. It is demonstrated that the semiblind algorithms outperform the conventional receiver in the low- and medium-speed area.

Index Terms—Alamouti coding, beamforming, semiblind channel estimation, space-time coding, steered space-time spreading, transmit diversity.

I. INTRODUCTION

In wireless communications, both widely and closely spaced antenna arrays offer some performance benefits in different environments. In the first case, open-loop transmit diversity schemes such as

Manuscript received November 8, 2004; revised August 10, 2005, and February 3, 2006. Part of this correspondence was presented at ICASSP, Philadelphia, PA, March 2005 [9]. The review of this paper was coordinated by Dr. K. Molnar.

A. M. Kuzminskiy is with the Lucent Technologies, Bell Laboratories, SN5 7DJ Swindon, U.K. (e-mail: ak9@lucent.com).

F. J. Mullany is with the Lucent Technologies, Bell Laboratories, Dublin 15, U.K. (e-mail: mullany@lucent.com).

C. B. Papadias is with Athens Information Technology, Athens, Greece (e-mail: papadias@ait.edu.gr).

Digital Object Identifier 10.1109/TVT.2006.878727